ChemPubSoc Europe

DOI: 10.1002/cctc.201900451

CHEMCATCHEM Full Papers

Catalytic Activation of Esterases by PEGylation for Polyester Synthesis

Jennifer Noro,[a] Tarsila G. Castro,[a] Filipa Gonçalves,[a] Artur Ribeiro,[a] Artur Cavaco-Paulo,*[a] and Carla Silva*[a]

In this work we explored PEGylation as an efficient strategy to improve esterase's catalytic performance. For this, we PEGylated three esterases, namely lipase from *Candida antarctica B* (CALB), lipase from *Thermomyces lanuginosus* (TL) and cutinase from *Fusarium solani pisi* (CUT) and evaluated their catalytic performance by using the biosynthesis of poly(ethylene glutarate) as model reaction. After PEGylation with a 5 kDa aldehyde-PEG, CALB and cutinase revealed an increase of activity against *p*-nitrophenyl butyrate hydrolysis (2-fold of increase for CALB and 4-fold of increase for cutinase). Unmodified and PEGylated lipase TL displayed however similar activity results. The polymerase activity of native and PEGylated esterases was also assessed. The data revealed a higher polymerase activity for the lipase TL and cutinase PEGylated forms (88% conversion for PEG-lipase TL and 34% for PEG-cutinase). Molecular dynamics were used to evaluate the effect of PEG on the geometry of the active site of enzymes with lid domain (TL and CALB). These studies corroborate the experimental data revealing a more open active site cavity for the PEGylated catalysts facilitating the catalysis.

Introduction

Protein PEGylation is the term attributed to the covalent bond formed between a protein and a unit of polyethylene glycol (PEG).[1] In the recent years, the PEGylation of proteins is being widely explored for many applications, due to their associated advantages. PEG is a nontoxic and nonimmunogenic polymer[2] already approved by FDA and classified as generally safe.[3]

The attachment of PEG to the surface of a protein or enzyme is a strategy often applied to improve its pharmacokinetic behaviour.[4] This modification results in several physical and chemical changes being the protein's size, the electrostatic binding, the conformation and hydrophobicity the main alterations associated.[2] It has been also described that PEGylation of enzymes may render them soluble in organic solvents maintaining however their catalytic activity.[5] Aiming to increase their stability, the PEGylation of proteins/enzymes is a current practice in the pharmaceutical industry, being some PEGylated-proteins currently available on the market.[1a]

Despite the improvement of protein's stability, PEGylation is commonly associated to a loss of activity. However, some contradictory examples are also possible to find in the literature. Vandertol-Vanier *et al.* observed that laccase from *Coriolopsis gallica* showed a higher catalytic activity than its native form when conjugated with mPEG.[6] Lee *et al.* PEGylated the interferon Beta-1b by site-specific PEGylation technology and increased their pharmacokinetic and antitumor activities.[7] Su *et al.* studied the effect of PEGylation of laccase from *Myceliophthora thermophila.* The authors observed an increment of the conversion and degree of polymerization when the PEGylated laccase was applied for catechol polymerization.[8]

The use of lipases for the catalysis of polyesters has been presented as an excellent alternative to the chemical approaches, generally involving the use of high temperatures and/or expensive and non-environmentally friendly metal catalysts.[9] Lipases are most often not expensive, reusable, and are associated to green chemistry practices.[10] Lipase from *Candida antarctica B* (CALB) is one of the most explored enzymes for the biosynthesis of polyesters[11] due to its unique specificities. The lack of need of interfacial activation and the diversity of solvent mediums in which reactions can be performed, are some of the most attractive properties associated.

Despite the broaden applications on several fields, the effect of PEGylation on esterase's activity and stability is still unexplored for synthetic purposes.

In this work, and for the first time, we PEGylated three esterases, namely lipase from *Candida antarctica B*, lipase from *Thermomyces lanuginosus* and cutinase from *Fusarium solani pisi* and evaluate their catalytic performance on the biosynthesis of poly(ethylene glutarate), from diethyl glutarate and ethylene glycol. The reactions were carried out in the absence of water using the substrates as reaction media. Molecular dynamics simulations in organic (reactant mixture) and aqueous medium were assessed in order to study the effect of PEGylation on the lipase's conformation and on the access of the substrate to the active site cavity. A complete characterization of the synthesized oligomers was performed by proton and carbon nuclear magnetic resonance spectroscopy (^{1}H and ^{13}C NMR), matrix-assisted laser desorption/ionization-time of flight (MALDI-TOF),

[a] *J. Noro, Dr. T. G. Castro, F. Gonçalves, Dr. A. Ribeiro, Prof. A. Cavaco-Paulo, Dr. C. Silva*
Center of Biological Engineering, University of Minho
Campus de Gualtar
4710-057 Braga (Portugal)
E-mail: artur@deb.uminho.pt
carla.silva@ceb.uminho.pt

Supporting information for this article is available on the WWW under https://doi.org/10.1002/cctc.201900451

Fourier-transform infrared spectroscopy (FTIR), differential scanning calorimetry (DSC) and thermogravimetric analysis (TGA).

Results and Discussion

PEGylation and Catalytic Properties of PEGylated Esterases

Most of the soluble enzymes are highly stabilized in the presence of high concentrations of polyethylene glycol. The presence of a medium with a high viscosity is expected to prevent the undesired changes in enzyme structure promoted by denaturing agents (e.g., high temperatures, strong basic conditions, extreme pH values) and, therefore, the stability of the soluble enzymes greatly increases. Based on these observations, our approach is to build such a layer around the enzyme to stabilize it, by PEGylation of the primary amine groups available.

The PEGylation of lipase from *Thermomyces lanuginosus* (lipase TL), lipase from *Candida antarctica B* (CALB) and cutinase from *Fusarium solani pisi* (CUT) was performed as reported in the literature, using an monofunctional PEG with an aldehyde group (MW 5000 Da).[12] The reaction occurred at acidic pH (5.1) in the presence of a reducing agent, sodium cyanoborohydride, as proposed in Scheme 1.

The TNBSA assay allowed the quantification of the free amine residues at the surface of the esterases which were not modified by PEGylation. Indirectly, we were able to infer that, under the conditions described, the PEGylation of CALB resulted in a protein with 100% of the exposed amines linked to PEG. After modification of lipase TL and cutinase, only 59 and 78% of the amino groups were linked to PEG, respectively (Table 1).

Table 1. Percentage of amine residues modified by PEGylation and activity of esterases, before and after PEGylation.

Esterase	Amine modification[a]	Activity[b] [U/$mg_{protein}$]
CALB	–	60
PEGylated-CALB	100%	132
Lipase TL	–	26
PEGylated-Lipase TL	59%	27
Cutinase	–	260
PEGylated-Cutinase	78%	1061

[a] Obtained by TNBSA assay. [b] Calculated by the hydrolysis of *p*-nitrophenyl butyrate over 1 min and considering the same initial amount of protein; 1 U of enzyme activity is defined as the amount of enzyme required to convert the substrate (*p*-nitrophenyl butyrate) into *p*-nitrophenol in 1 min.

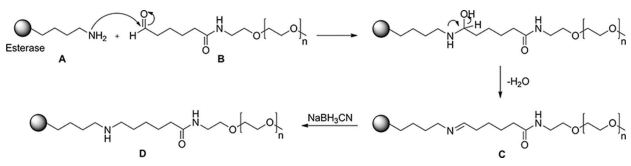

Scheme 1. Proposed mechanism for the PEGylation of esterases; A) Lysine residue of esterase; B) PEG-Aldehyde; C) Esterase-lysine-PEG as imine intermediate; D) Esterase-lysine-PEG.

Depending on the position of the amine residues at the enzyme's surface, stereo-chemical impediments might influence the degree of PEGylation. More exposed amines are more prone to covalently react with the PEG available chains.[13] Regarding the methodology used to PEGylate, it is likely that the amine residue of the *N*-terminus had been also PEGylated. This assumption is based on the use of acidic pH during the reaction, which led to the activation of the *N*-terminus.[12]

The PEGylation was also ascertained by SDS-PAGE electrophoresis as a complementary methodology (Figure 1).

Lipase from *Thermomyces lanuginosus* has a typical visible band at 30 kDa and when PEGylated a new band appears at around 40 kDa (corresponding to 2 units of PEG covalently bond to the protein). Cutinase display a representative band at 22 kDa, while its PEGylated form shows an intense smear with two pronounced bands in the range of 25 and 45 kDa. The PEGylated forms present also an evident smear suggestive of an increase of the molecular weight incremented by PEGylation. As a consequence of the reduction in the number of free amino groups, the enzyme derivatives (PEGylated forms) showed a smaller electrophoretic mobility toward the cathode than the unmodified esterase.

Due to the presence of stabilizers in the medium, the native and PEGylated CALB were not successfully revealed by SDS-PAGE electrophoresis.

The activity of enzymes is a parameter greatly influenced by the PEGylation procedure. Thus, the hydrolytic activity of the esterases against *p*-nitrophenyl butyrate was evaluated, before and after PEGylation, and the results obtained reveal a different catalytic behaviour of the catalysts after the chemical modification. We have found that PEGylation greatly enhanced the CALB and CUT catalytic activities comparing to their native state. This was a surprising result since only few examples of increased activity after PEGylation can be found in the literature, as previously mentioned.[6] Comparing to their native forms, the activities of PEGylated CALB and CUT increased 2-fold and 4-fold after PEGylation, respectively. According to our data, the PEGylation of lipase TL did not influence its catalytic activity which remained unaltered after chemical modification.

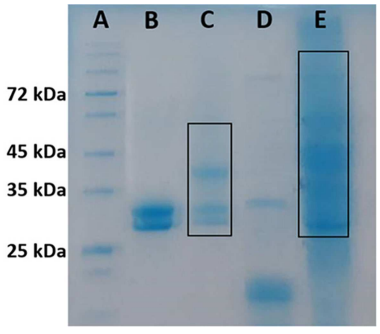

Figure 1. SDS-PAGE gel of native and PEGylated esterases stained with Coomassie brilliant blue; **A**: GRS Protein Marker Blue (from Grisp, Portugal), **B**: Lipase from *Thermomyces lanuginosus*; **C**: PEGylated lipase from *Thermomyces lanuginosus*; **D**: Cutinase from *Fusarium solani pisi*; E: PEGylated cutinase from *Fusarium solani pisi*.

The addition of free PEG to the native enzymes was also evaluated and the results revealed no effect of the stabilizer on their hydrolytic activity (data not shown).

It is noteworthy that all PEGylated catalysts remained stable for at least six months of storage at room temperature.

To evaluate their stability under processing conditions, we incubated the enzymes at 40 °C and measured the activity over time (activity measured using *p*-NPB as substrate). From the results obtained one might infer that PEGylation conferred stabilizing effects to the modified esterases. We observe that both native and PEGylated enzyme forms, remained active for more than 50 days under the same storage conditions, with a minimal activity loss. During the process at 40 °C, no loss of activity is registered based on the results obtained after 8 h of incubation (Figure 2). The temperature of incubation has been described in literature as a differential factor for PEG stabilization performance. The high thermal stability achieved herein at 40 °C might be explained by the high viscosity of PEG layers surrounding the enzymes.

Although PEGylation is being described as a methodology prone to inactivate some proteins,[14] the results obtained clearly demonstrate that this methodology allows to improve esterase's activity and stability.

Circular dichroism (CD) was also accessed to evaluate the structural changes induced by PEGylation (Figure S1). Comparing with native enzyme forms, a lower signal intensity of the spectra was observed for all the PEGylated esterases. These results are commonly associated to a slight unfolding of the structure.[15] The lower intensity of the spectra might also be associated with the concentration of the samples, which was calculated based on the average MW, possibly inducing intensity variations. Moreover, and according to SDS-PAGE and TNBSA results, the esterases are PEGylated differently (CALB > CUT > TL), displaying thus variations on the CD spectral intensity signal. Despite the differences observed on the signal intensities, the CD curves of both native and PEGylated enzymes display a typical enzyme spectra, revealing no major conformational changes after PEGylation. The CD spectra obtained for CALB and PEG-CALB has a different profile as described in literature. As confirmed previously, no SDS-PAGE could be obtained for these enzymes, due to the presence of high amount of stabilizers, which might also hinder the proper acquisition of the CD spectra. Considering this, and for a better clarification about the effect of PEG on the esterases conformation, we performed molecular dynamic simulation studies.

The ability of esterases to act as polymerases is being widely studied, however the effect of PEGylation on their catalysis performance is still unexplored. Alongside with their hydrolytic activity, the main purpose of the work was to evaluate the catalytic performance of the modified esterases on the biosynthesis of an aliphatic polyester, poly(ethylene glutarate).

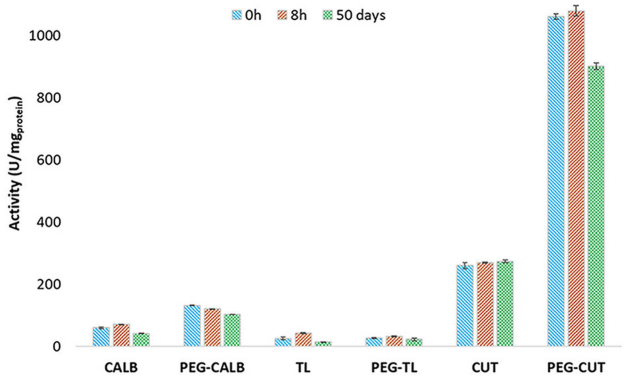

Figure 2. Absolute activity of esterases (native and PEGylated forms), at time zero, after 8 h, and after 50 days of incubation at 40 °C in phosphate buffer (pH 7.8). The activity was measured against *p*-NPB over 1 min and considering the same initial amount of protein; 1 U of enzyme activity is defined as the amount of enzyme required to convert the substrate (*p*-nitrophenyl butyrate) into *p*-nitrophenol in 1 min.

Effect of PEGylation on the Polymerase Activity of Esterases

The synthesis of poly(ethylene glutarate) catalysed by immobilized CALB was previously investigated by us,[16] using diethyl glutarate and ethylene glycol diacetate as starting reagents. Herein, we replace the ethylene glycol diacetate by ethylene glycol, which would allow to obtain a greener sub-product, ethanol, instead of ethyl acetate. A greener and environmentally friendly methodology is also associated with the proposed method due to the absence of solvents on the reaction mixture, being all the reactions carried out in bulk. Moreover, mild reaction conditions of temperature (40 °C) and short reaction times were used, reducing therefore the energy costs associated to the process.

Regarding the previous results published[16] we proceed with the processing optimizations (data not shown) and established the best reaction conditions for the polymerization of the proposed polyester: 2 h under ultrasound (US) followed by 5 h under vacuum at 40 °C, following the reaction presented in Scheme 2.

Considering the optimized reaction procedure, the enzyme loading (2 to 130 U/mg) was tested to evaluate the best conditions to attain the highest synthesis conversion (Figure S2).

Results from Figure S2 reveal that, when comparing to their native forms, the highest product conversion is obtained when using both PEGylated-lipase TL and PEGylated-CUT enzymes. CALB display however an opposite behaviour after PEGylation, giving rise to slightly lower conversion levels. One can also observe that all enzymes tested show a similar trend between 2 and 130 U/mg of enzyme loading, reaching however different levels of conversion, depending on the enzyme form and source. At the maximum enzyme loading, PEGylated lipase TL reveal the highest polymerase performance comparing to its

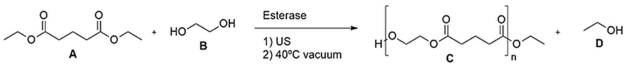

Scheme 2. Synthesis of poly(ethylene glutarate) catalysed by esterase; A) diethyl glutarate; B) ethylene glycol; C) poly(ethylene glutarate); D) ethanol.

native form, reaching levels of conversion of around 90% whereas PEGylated-CUT converts only 60% of the monomers. The reactions were also carried out with native enzymes in the presence of free PEG in the reaction medium. The data obtained at these conditions showed lower conversions than compared with native enzymes without additive (data not shown). In this case, the free PEG can saturate the medium, hindering the access of the substrate to the enzymes' active site, while when PEG is attached to the enzymes, it induces an opposite effect, contributing to the improvement of their activity and stability.

Comparing the polymerase results with the hydrolytic activity, the findings indicate that for lipase TL the presence of PEG chains on the macromolecular surface somewhat maintain unaltered the binding of *p*-NPB, a more hydrophilic substrate, however increasing considerably the binding of the hydrophobic starting reactants. Apparently, PEG modification improved the relative selectivity of the enzyme towards different substrates. For a better understanding of the role of PEG on the performance of the modified esterases, we calculated the degree of polymerization (DP) and oligomer conversion obtained when using a fixed enzyme loading (65 U/mg) (Figure 3).

Comparing to its native form, PEGylated-TL showed the highest biosynthesis activity (60% of improvement) evaluated in terms of average DP (conversion 88%; DP_{avg}: 6 units). Both CALB forms, native and PEGylated, converted similar amount of starting reagents into poly(ethylene glutarate) with similar DP. The PEGylated form of cutinase was more prone to catalyse the polyester synthesis than its native form (20% conversion) however with a corresponding DP lower than the obtained when using PEGylated TL.

Many reports using CALB as catalyst for the polyester synthesis are found in literature, however the use of native lipase TL for this purpose is still poorly explored. Zhao *et al.*,[17] reported the *in situ* coating of cotton with polyesters synthesised by lipase TL and CALB. In their work the polyester synthesis was carried out using different amounts of each enzyme, and for this reason it was hard to distinguish their catalytic behaviour for the same substrate. Nevertheless, the findings suggested lower catalytic performance of lipase TL regarding polyester biosynthesis.

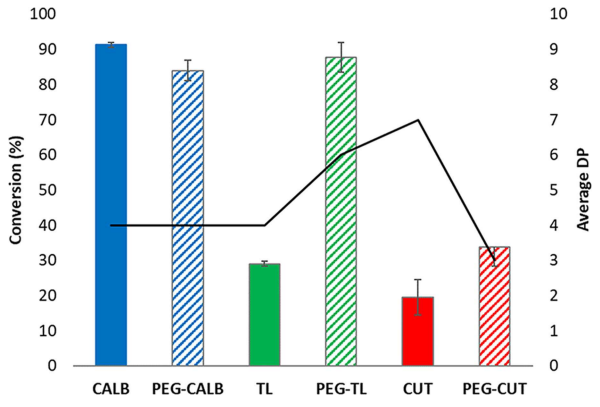

Figure 3. Conversion (%) and degree of polymerization (DP) for all the tested esterases under the optimized conditions: 2 h under US followed by 5 h under vacuum, at 40 °C; 65 U/mg. The bar graph corresponds to the conversion (%) and the line graph to the average DP.

Naik *et al.*,[18] studied the specificity of different ester groups for different lipases. Their findings recognized a different catalytic behaviour for CALB and lipase TL. While CALB had a large acyl binding cleft with a narrow alcohol binding cleft, lipase TL presented a wide alcohol binding cleft, and a narrow cleft for acyl binding.

These assumptions suggest that the use of a large acyl compound (like diethyl glutarate) might favour the reaction when CALB is applied. Moreover, being the ethylene glycol a small molecule, more easily gets into the enzyme's alcohol cleft. These findings are in accordance with the high conversion obtained for either native and PEGylated CALB (>80%).

For lipase TL, the opposite is expected to occur. The large alcohol cleft and the narrow acyl cleft may justify the low conversion obtained for the native form (<30%). The size of the starting reagents may hinder the access to the respective enzyme clefts, which is mitigated by the presence of PEG on PEGylated enzyme form, which in turned higher polymerase conversion.

From all the esterases tested, cutinase presented the lowest catalytic performance on the polyester biosynthesis giving rise to conversion below 33%. Despite the low conversion, this esterase was able to catalyse the synthesis of larger oligomers, revealed by the highest oligomer DP observed (DP_{avg}: 7 units). The studies of Naik *et al.*,[18] reveal that cutinase from *Fusarium solani pisi* have both clefts larger, which may justify the higher DP obtained when this catalyst was used.

Both, lipase and cutinase, belong to the same family of α/β hydrolases, but display different affinities to the substrates.[19] While the activity of lipase is greatly enhanced at lipid-water interface, needing interfacial activation, cutinase lack this need of activation.[19] This phenomenon is crucial for lipases to exhibit activity, since they possess a hydrophobic flap in their structure which overlies the active site and changes in this flap are related to the interfacial activation.[20] In lipase TL the need for this activation is reported, while CALB only needs little or even no activation.[18] Considering these assumptions, one might infer that on the presented experiments the need of interfacial activation of native lipase TL might led to a lower polyester biosynthesis performance, when compared with CALB.

We believe that the higher polymerase activity observed for PEGylated lipase TL might be attributed to the PEG linked to the enzyme's surface. The polyethylene glycol chains can change the structure of the flap or the global enzyme conformation. The linked PEG may enlarge the active site or create a larger opening for an easier access of the substrates. Moreover, the results obtained can also be explained by entropic stabilization by PEG conjugation due to the restricted motion of some surface amino acid side chains, resulting in a more stable active site. Thus, in order to better understand the role of PEG on the improvement of the catalytic performance of lipase TL and CALB, molecular dynamics (MD) simulations were conducted.

Molecular Dynamics Simulations

MD simulations were carried out for lipase TL, CALB and all analogues (Figure S3) to examine their behaviour near the active site and lid, when in an aqueous medium or in substrates medium, before and after PEGylation. Regarding the similar conversion levels obtained for both native and PEGylated cutinase and the lack of interfacial activation, no MD simulations were conducted. The small differences obtained experimentally are easily explained by the enzyme large clefts which did not favour the synthesis when either native or PEGylated forms are used.

In the case of lipase TL, PEGylation was thought to replace up to 5 Lys per LYP (PEGylated Lys), as it was experimentally confirmed by the TNBSA assay an average of 5 PEGylated Lysines. The PEGylation of Lys98, which is placed in one of the enzyme's arms that can move the lid, was also assessed. For PEGylated-CALB, and since experimentally all the Lys were PEGylated, all the 9 lysines were replaced by LYP.

The lid of lipase TL comprises the amino acids 82–98, presenting an α-helix (residues 86–91) and two hinge domains (anterior and posterior). The catalytic triad is composed of Ser146, His258, and Asp201 residues, and as this lipase approaches a lipid interface, the lid moves, clearing the access to the catalytic triad and allowing catalysis.[21] In the case of CALB, the catalytic triad is formed by the Ser146, His224 and Asp187 residues and, similarly to lipase TL, there is an α-helix situated above the cavity that encompasses the triad (residues 139–148). However, in this lipase the access to the active site is not hampered as in the case of lipase TL. In fact, several authors do not consider this helix as a lid, and therefore the catalytic mechanism is not dependent on the displacement of this structure.[22]

Despite the mechanistic differences already established for both lipases, these assumptions are not sufficient to explain the differentiated results obtained experimentally, especially for the PEGylated enzyme forms. The aim of these modelling studies is to understand the role of the medium and of the PEGylation on the triad cavity and on the lid or lid-like structure, in the case of CALB. RMSD results (Figure S4) demonstrate that in both medium (water or reactants) lipase TL and analogues are very stable, varying only 0.15–0.4 nm from the initial X-ray structure. For CALB systems, a smaller deviation is observed, ranging from 0.1–0.3 nm. However, it is noteworthy that the PEG stabilizing effect is only observed when the systems are in the solvent-reactants mixture, being much less pronounced in water.

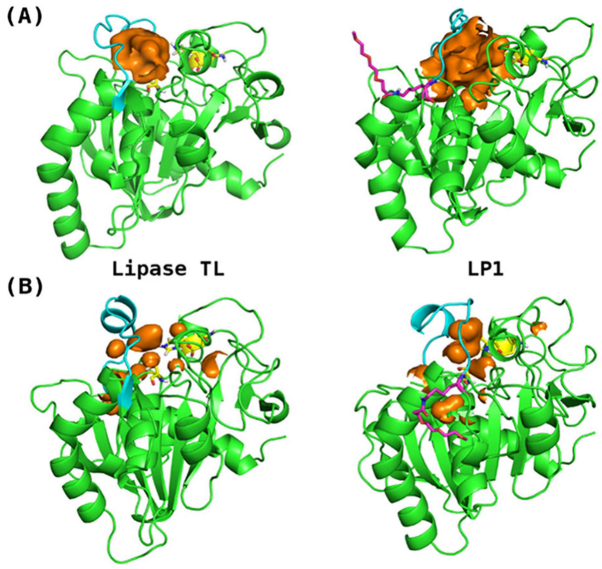

Figure 4. Middle conformations of lipase TL and PEGylated analogue LP1, in reactant mixture (A) and in water (B), highlighting the interior cavities and pockets surrounding the catalytic triad and lid regions.

After simulation, the middle conformation was determined for each case-studies, to evaluate the effects of the medium and PEGylation on the global width of the cavity that encompasses the catalytic triad. Although these lipases are globally stable structures, when looking to the central structures (Figure 4 and Figure S5), the most significant deviations observed are in the region of the lid structure.

The effect of medium and PEGylation is exemplified in Figure 4, by Lipase TL and LP1 analogue (LYP in position 98), where it is perceptible that wild type lipase TL and the antilog, in reactants mixture, present a larger cavity in comparison with the same systems in water. Also, this example indicates that the PEGylation of the Lys98 favours the enlargement of the enzyme's active centre. A larger cavity can result in a larger acyl cleft, which led to a better accommodation of diethyl glutarate. This is evident in Figure 4 (A), which highlights the active centre of Lipase TL and LP1 in reactant mixture. Additional Figure in SI (Figure S5), shows the cavities for the other analogues, some measurements and surface representation, that helps to perceive a greater access to the catalytic triad of PEGylated forms of the analogues comparing with the access to the wild type form.

The CALB middle structures demonstrate that the medium has a similar impact on the enzyme's cavity region. In water, the PEGylation seems to not disturb the structure and the active site cavity remain unaltered. In the reactant mixture (Figure 5A), although PEG stabilizes CALB, it does not generate a great enlargement of the cavity, promoting a more discrete effect on this enzyme when compared with the effect towards TL. Regarding the similar conversion and DP obtained experimentally for both CALB forms, a negligible effect of PEG on the CALB structure was expected. CALB possesses a large acyl cleft and a small alcohol cleft, ideal for the polymerization of the substrates tested. MS studies reveal that PEG did not disturbed the active site, thus maintaining the size of both clefts which resulted in similar oligomer conversion, independently on the enzyme form used.

Recently, MD studies and other modelling techniques have been used to help understand the mechanisms of interfacial activation in lipase TL, CALB and other lipases.[23] However, these studies are in general performed in water medium, or in a water-lipid/water-oil interface. We show herein an innovative way to demonstrate the contribution of enzyme PEGylation on the final enzyme arrangement. By comparing simulations in water and in the reactant mixture, we were able to confirm that the starting organic reactants, diethyl glutarate and ethylene glycol, create the best environment to enhance the catalytic properties of lipase, i.e., an open access to the catalytic triad.

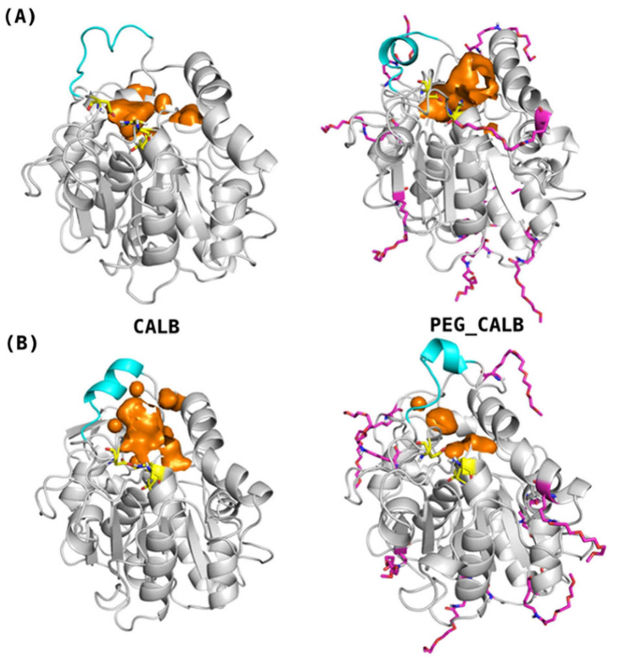

Figure 5. Middle conformations of CALB and PEGylated CALB, in reactant mixture (A) and in water (B), highlighting the cavities and pockets surrounding the catalytic triad and lid regions. Cartoon in grey, catalytic triad in yellow, lid-like region in cyan, LYP residues in magenta and the orange spheres represent the empty space (cavity or pocket) on each structure.

Poly(Ethylene Glutarate) Characterization

The results of the biosynthesis with all the esterases are summarized in Table 2, including the number average molecular weight (M_n) the weight average molecular weight (M_w), the polydispersity index (M_w/M_n) and the average and maximum degree of polymerization, for all the reactions performed.

The synthesized oligomers display (M_n) values between 415.97 and 799.99 g/mol, and (M_w) values between 527.03 and 1031.61 g/mol. All reactions gave rise to oligomers with good polydispersity, being PEGylated-CALB the more homogeneous (1.04) and PEGylated-TL the more heterogeneous (1.48).

As previously stated, PEGylated-lipase TL showed higher DP than its native form. This PEGylated esterase, also showed the highest maximum degree of polymerization (16 units). Both forms of CALB have the same average and maximum DP. The native form of cutinase showed better performance than its PEGylated form. A possible explanation for all these results was already discussed elsewhere in this paper.

NMR^{1}H NMR spectra of the new oligomers formed have a similar pattern independently on the enzyme used and the degree of polymerization obtained. In Figure 6 is represented the ^{1}H NMR spectra of poly(ethylene glutarate). The monomer, ethylene glycol, presents only one peak in the spectrum which appears at δ_H 3.73 ppm. These protons, suffer a significant chemical shift when

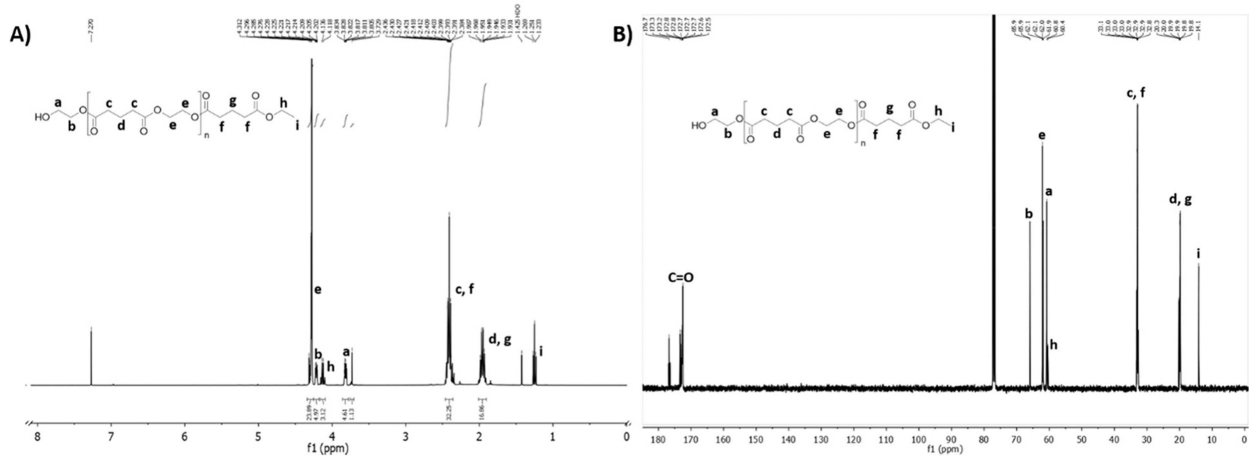

Figure 6. ^{1}H (A) and ^{13}C (B) NMR spectra of poly(ethylene glutarate) with a conversion of 95%, recorded in $CDCl_3$.

Table 2. Number average molecular weight (M_n) and weight average molecular weight (M_w), polydispersity (PDI), average degree of polymerization (DP_{avg}), maximum degree of polymerization (DP_{max}) (calculated by MALDI-TOF) and conversion (%) after poly(ethylene glutarate) biosynthesis after 2 h under ultrasound followed by 5 h under vacuum at 40 °C with 65 U/mg of enzyme.

Esterase	M_n	M_w	M_w/M_n	DP_{avg}	DP_{max}	Conversion [%] (by ^{1}H NMR)
CALB	580.89	625.18	1.08	4	8	91.3 ± 1.3
PEGylated-CALB	597.91	624.32	1.04	4	8	84.0 ± 5.9
Lipase TL	415.97	590.78	1.42	4	10	29.0 ± 1.4
PEGylated-Lipase TL	691.49	1021.40	1.48	6	16	87.8 ± 8.7
Cutinase	799.99	1031.61	1.29	7	15	19.6 ± 16
PEGylated-Cutinase	428.02	527.03	1.23	3	8	33.9 ± 13

the synthesis occurred, appearing as a singlet at δ_H 4.30 ppm (**e**). The terminal ethylene glycol unit (protons **a** and **b**) appeared as two distinct peaks, one at δ_H 3.82 ppm (protons **a**) and the other at δ_H 4.21 ppm (protons **b**), both as multiplets. Glutarate moiety in the oligomer did not show significant changes comparing with the same protons in the monomer. Only the terminal part (protons **h** and **i**) showed a decrease in the signal intensity depending on the degree of polymerization. In ^{13}C NMR spectra (Figure 6B) the expectable peaks respecting to the new oligomers are observed. The C=O are observed between δ_C 172.5 and 176.9 ppm. The terminal CH_3 (**i**) appears as δ_C 14.1 ppm and CH_2 (**h**) at δ_C 60.4 ppm, while the other carbons of the glutarate (**c**, **d**, **f**, **g**) moiety are observed between δ_C 19.8–20.3 and 32.7-33.3 ppm. The ethylene glycol moiety (**e**) appears at δ_C 61.9 and 62.1 ppm. The terminal **a** and **b** carbons are observed at δ_C 60.9 and 65.9 ppm, respectively. Other complementary spectra (DEPT, HSQC and HMBC) can be found in the supporting information of this paper (Figures S6–S8).

The pattern obtained was in accordance to the previous poly(ethylene glutarate) reported,[16] and the chemical shifts in the ^{13}C NMR are typical of polyesters.[24]

MALDI-TOF

The MALDI-TOF mass spectrum, recorded in linear positive mode, of the formed poly(ethylene glutarate) display a typical isotopic distribution between 500 and 2500 *m/z* (Figure 7). From the spectra one can depict a repetition unit mass between each two peaks, corresponding to the monomeric repeating unit ([M] = 158), and confirming its presence in the oligomer main chain. Similar spectra were obtained for the polyester synthesized by the other esterases applied, showing different DPs (data not shown).

These results agree with the formation of the proposed oligomer, with $DP_{avg} = 5$, as suggested by ^1H NMR and ^{13}C NMR data. The pattern obtained for the polyester is in accordance with similar polyesters described in the literature.[25]

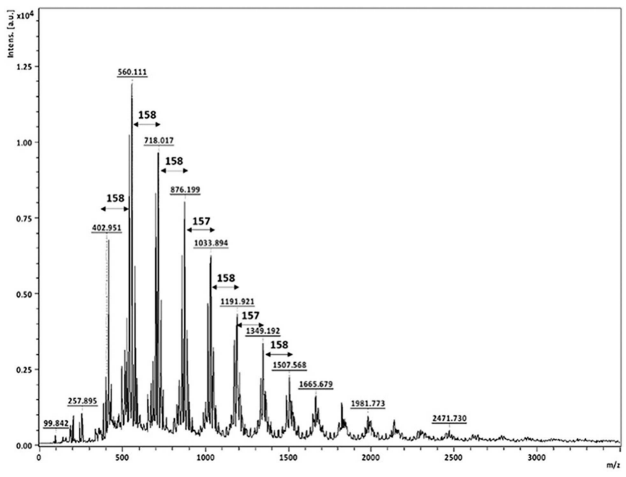

Figure 7. Positive ion MALDI-TOF spectra of poly(ethylene glutarate) ($DP_{max} = 16$ and $DP_{avg} = 5$).

FTIR, DSC and TGA

FTIR analysis was also conducted to evaluate the chemical changes after enzymatic synthesis. From the data obtained (Figure S9), as expected, one can observe that the stretch of the OH terminal group is more pronounced for low degrees of polymerization. Also, the OH appears in the oligomer at ν 3500 cm^{-1} while in the monomer is observed at ν 3300 cm^{-1}. Regarding the C=O bond, it is observed at ν 1700 cm^{-1} for monomers and oligomers.

The glass transition temperature (T_g) of the oligomer was determined by DSC analysis. Poly(ethylene glutarate) showed a value of $T_g = 77.29 \pm 1.21\,^{\circ}C$ with an energy of $\Delta C_p = 0.228 \pm 0.095$ J/g $^{\circ}C^{-1}$ (Figure S10). A melting point (T_m) is observed at $T_m = 195.7\,^{\circ}C$ with an associated enthalpy of $\Delta H_m = 19.967$ J/g. The pattern here obtained is very similar to the DSC analysis of polyesters reported in literature.[24] None of the monomers showed thermal events at the same temperature range of the oligomer spectrum, as depicted in Figure S10.

The thermal properties of the synthesized polyester were investigated by thermogravimetric analysis scanned between 30–800 °C (Figure S11). Both monomers present a one-step decomposition, losing all weight at around 180 °C. The oligomer presents two distinct stages of weight loss: one at around 220 °C, corresponding to 10% of weight loss; and another at 400 °C, corresponding to 50% of weight loss. The total material decomposition was observed near 500 °C. The thermal behaviour observed, typical for this type of oligomers,[26] confirms the polyester biosynthesis.

Conclusions

In this work we PEGylated three esterases and compared their catalytic performance for the biosynthesis of poly(ethylene glutarate). All the enzymes were successfully PEGylated, and their hydrolytic activity, with exception of lipase TL, was improved comparing to their native form. Regarding their polymerase activity, we observed a similar performance for native and PEGylated CALB, explained mainly by its large acyl cleft. On the other hand, lipase TL presented an improved performance when PEGylated. Molecular dynamics simulations, performed on lipase TL and CALB, support that the PEGylation of the lysine at the enzyme's lid had a positive effect on the substrate accessibility to the active site of the catalyst. The simulations conducted in the reactant mixture medium confirm the stabilization of the enzyme by PEG in a more organic environment. The entropic stabilization by PEG conjugation also caused the motion restriction of some surface amino acid side chains, resulting in a more stable active site.

PEGylation of esterases demonstrated to be an easy, not expensive and timeless methodology to enhance enzyme's

performance on the biosynthesis of polyesters, envisaging a diverse range of applications.

Experimental Section

Materials and Methods

Materials

Lipase from *Thermomyces lanuginosus* (solution, ≥100,000 U/g), lipase from *Candida antarctica* B (0.3 U/mg), *O*-[2-(6-Oxocaproylamino)ethyl]-*O'*-methylpolyethylene glycol (PEG, MW 5000 Da), ethylene glycol (≥99%), diethyl glutarate (≥99%), 2,4,6-trinitrobenzene sulfonic acid (5% (w/v) in H_2O), *p*-nitrophenyl butyrate (*p*-NPB, ≥98%) and sodium cyanoborohydride (95%) were purchased from Sigma-Aldrich. Tetrahydrofuran (HPLC grade, Fisher Chemical) was used without further purification. Ultrafiltration was performed with Ultracel 10 kDa regenerated cellulose ultrafiltration discs, 47 mm (Millipore) with ultrapure water (Milli-Q). The expression and production of cutinase from *Fusarium solani pisi* (EC 3.1.1.74) was performed following the procedure reported by Araújo *et al.*[27]

Enzyme Characterization

SDS-PAGE

SDS-PAGE electrophoresis of lyophilized esterases was performed by solubilizing them in water and loading on polyacrylamide Gel Electrophoresis (SDS-PAGE) gel 12.5%. The gel was stained with Coomassie brilliant blue solution to analyse size and purity.

Esterase Activity

The activity of all the esterases was determined by a continuous spectrophotometric assay using *p*-nitrophenyl butyrate (*p*-NPB) as substrate. One unit of enzyme activity is defined as the amount of enzyme which catalyses the production of 1 μmol *p*-nitrophenol per minute. The standard assay was performed at 37 °C in a final volume of 4 mL containing *p*-NPB (6 mM), the enzyme and the assay buffer (K_2HPO_4 buffer, pH 7.8, 50 mM). The reaction was initiated by the addition of the enzyme. The hydrolysis of *p*-NPB was monitored by the formation of the *p*-nitrophenol at 400 nm.[28] The measurements were conducted in a Synergy Mx Multi-Mode Reader from BioTek (USA).

Protein quantification

The quantification of the protein concentration was performed by using the DC protein assay (BIO-RAD).

Degree of PEGylation

The degree of enzyme PEGylation was indirectly evaluated by colorimetric titration. This methodology occurs by the reaction of 2,4,6-trinitrobenzene sulfonic acid (TNBSA) with the free amine residues at the surface of the enzymes. Knowing the total amount of amine residues available in each protein, this quantification allowed us to calculate the amount of PEG chains coupled to each esterase. The procedure was followed as reported by Castillo *et al.*[29]

Circular Dichroism

The native and modified esterases were studied by circular dichroism spectroscopy, using a Jasco J-1500 spectropolarimeter, equipped with a temperature controller set at 37 °C. The enzyme concentration was set at 5 μM dissolved in a potassium phosphate buffer (5 mM, pH 7.5). The baseline was recorded using the same buffer and subtracted to the enzyme spectra. The spectra were recorded between 185–260 nm at a scan speed of 20 nm/min and bandwidth of 1 nm. The path-length cell was 1 mm. The final spectra were obtained by the average of three scans for each sample.

Molecular Dynamics Simulations

Molecular Dynamics (MD) simulations were performed on lipase from *Thermomyces lanuginosus* (lipase TL, PDB ID: 1TIB),[30] on lipase B from *Candida antarctica* (CALB, PBD ID: 1TCA),[31] and on its PEGylated forms, to understand the role of PEG on the lid and on the active site cavities, under different environments.

Lipases were modelled in the simple point charge (SPC) water model, for control, and in a mixture of diethyl glutarate and ethylene glycol (reactant mixture), using the same proportion as experimentally. In both cases, a cubic box with an approximate volume of 530 nm^3 was used, with the enzyme centralized and Na^+ ions to neutralize the system. One stage of energy minimization was performed using a maximum of 50,000 steps with steepest descent algorithm. Position restraints (with force constant of 1000 $kJ \cdot mol^{-1} \cdot nm^{-2}$) were applied to all heavy atoms at the initialization steps, the first using an NVT ensemble and the second, with NPT. The temperature was maintained constant with V-rescale algorithm[32] and the pressure, was regulated at 1 atm, with the Parrinello-Rahman barostat.[33] In the control simulation (enzyme in water), a temperature of 310 K was used, but for the experiment simulation(enzymes in reactant mixture)), a temperature of 313 K was chosen, to mimic the experimental procedure. The following coupling constants were considered: $\tau_T = 0.10$ ps and $\tau_P = 2.0$ ps. After that, all systems were submitted to MD simulations during 40 ns, in an NPT ensemble, without position restraints.

All simulations were performed using the GROMACS 5.1.4 version,[34] within the GROMOS 54a7 force field (FF).[35] The Lennard-Jones interactions were truncated at 1.4 nm and the particle-mesh Ewald (PME)[36] method for electrostatic interactions with a cut-off of 1.4 nm was used. The algorithm LINCS[37] was used to constrain the chemical bonds of the proteins as well as the algorithm SETTLE[38] in the case of water.

To design and simulate the box containing the substrates diethyl glutarate and ethylene glycol as solvents, the parameterization of these molecules was optimized. For this a PM6 calculation[39] with Gaussian09 software[40] was run followed by submission of the resulting optimized structures at ATB server (Automated Force Field Topology Builder).[41] As result, optimized structures were obtained with a GROMOS 54a7 FF parameter associated to each one.

The PEGylated systems were designed replacing Lysine (Lys) residues to a new type of Lysine, named as LYP, where a PEG chain is linked. To prevent high computational costs, only three PEG units were connected to each chosen lysine side chain. The GROMOS topology necessary for this new residue, LYP, was also obtained using ATB server. In the case of lipase TL, 5 types of PEGylation took place until the limit of 5 of 7 Lys PEGylated: the analogue LP1 has LYP only in position 98, LP2 has LYP98 and the Lys PEGylated in β-sheets (positions 74, 223 and 237), LP3 has LYP98 and the Lys PEGylated in α-helices (positions 24, 46 and 127), LP4 present LYP98 and 4 random Lys PEGylated (positions 24, 46, 223 and 237) and LP5 is the only case where Lys98 was not PEGylated, but 5 random Lys were replaced by

LYP (positions 46, 74, 127, 223 and 237). For CALB, an analogue with all Lys PEGylated was designed. This was done to correspond to the results obtained experimentally. Figure S1 (see supporting information) shows the PEGylation strategy.

From MD simulations, a cluster analysis was computed from GROMACS package, with the single-linkage method, to determine the middle structure of each enzyme, i.e., this technique adds structures that are below a RMSD cut-off, generating more or less populated clusters and, within the largest cluster, it finds a middle structure that is the most representative of the whole simulation. The changes in the lid conformation and in the region involving the catalytic triad were followed through visualization analysis with PyMOL.[42]

NMR

All NMR spectra, namely ^{1}H NMR, ^{13}C NMR, Distortionless Enhancement by Polarization Transfer (DEPT), ^{1}H-^{13}C Heteronuclear Single Quantum Coherence (HSQC) and ^{1}H-^{13}C Heteronuclear Multiple Bond Correlation (HMBC) were carried out on a Bruker Avance III 400 spectrometer (400 MHz for ^{1}H and 100 MHz for ^{13}C). Deuterated chloroform ($CDCl_3$, Cortecnet, France) was used as NMR solvent, and the peak solvent used as internal reference. Signal multiplicity are given as: s (singlet), t (triplet), q (quartet) and m (multiplet).

MALDI-TOF

MALDI-TOF mass spectra were acquired on a Bruker Autoflex Speed instrument (Bruker Daltonics GmbH) equipped with a 337 nm nitrogen laser. The procedure was followed as previously reported.[43] 2,5-dihydroxybenzoic acid (DHB) or α-cyano-4-hydroxycinnamic acid (CHCA) were used as matrix. Samples were analysed in the linear positive or negative mode.

The number average (M_n) and weight average molecular weight (M_w), the polydispersity index (PDI = (M_w/M_n)), the average and maximum degree of polymerization (DP_{avg}, DP_{max}) (DP_{avg} = *Mw*/repeating unit of the oligomer) were calculated based on the MALDI-TOF spectra obtained, based on the *m/z* values and intensity, following Equations (1) and (2):

$$M_n = \frac{\Sigma niMi}{\Sigma ni} \quad (1)$$

$$M_w = \frac{\Sigma niMi^2}{\Sigma niMi} \quad (2)$$

Where *ni* is the relative abundance of each peak in the MALDI-TOF spectra and *Mi* is the *m/z* corresponding to each peak.

FTIR

Infrared spectra were recorded on a FTIR Bomem MB using NaCl cells. The samples were analysed over the range 500–4000 cm^{-1}, with a spectral resolution of 4 cm^{-1}. All spectra were an average of over 20 scans.

DSC

Differential scanning calorimetry (DSC) measurements were conducted on a power-compensated DSC instrument (DSC 6000 Perkin Elmer) with a nitrogen flux of 20 mL/min, using stainless steel capsules in the temperature range of 20–250 °C (heating rate: 20 °C/min, sample weight: 2–3 mg). The DSC device was calibrated using indium and zinc, both of high purity. The samples were freeze-dried, prior to the analyses and the sample was measured at least six times, to validate the results.

TGA

Thermogravimetric analysis (TGA) analysis was performed in a Perkin Elmer TGA 4000. The calibration was performed with metals, such as Nickel, Alumel and Perkalloy, based on their Curie Point Reference. The temperature range was 30–800 °C (heating rate 20 °C/min, sample weight: 12–16 mg) and the nitrogen flow rate was 20 mL/min (3 bar).

General Procedure for the PEGylation of Esterases

The PEGylation of the esterases was performed using the procedure reported by Mayolo-Deloisa *et al.*[12] Briefly, the esterase (12 mg/mL) was solubilized in phosphate (100 mM) and $NaBH_3CN$ (20 mM) buffer (pH = 5.1) followed by the addition of the PEG-aldehyde (esterase 1 : 4 PEG w/w). The reaction mixture was placed at 4 °C, overnight, under stirring. The separation of the unreacted PEG and buffer was carried out by ultrafiltration using a 10 kDa regenerated cellulose membrane housed in an ultrafiltration device using ultrapure water. The PEGylated esterase was obtained as a white solid after freeze-drying for 2 days.

General Procedure for Synthesis of Poly(Ethylene Glutarate)

Ethylene glycol was added to a 50 mL round-bottom flask, followed by the addition of the diethyl glutarate (equimolar amount) forming a biphasic mixture. The esterase was added, and the suspension was placed in an ultrasonic bath (USC600TH, VWR International Ltd., USA; frequency 45 kHz and power of 120 W) programmed to not exceed the 45 °C. After sonication for 2 hours, the round-bottom flask was transferred to a rotary evaporator (Heidolph, Germany) at 40 °C, 120 rpm, to complete 7 hours of total reaction time. Tetrahydrofuran was added to the reaction mixture and the enzyme was removed by filtration. The solvent was removed in the rotary evaporator and the final solution formed a colourless oil.

^{1}H NMR ($CDCl_3$): δ_H 1.23 (t, J = 6.8 Hz, CH_3), 1.91–1.96 (m, CH_2), 2.37–2.42 (m, CH_2), 3.78-3.81 (m, CH_2), 4.10 (q, J = 7.2 Hz, CH_2), 4.18–4.20 (m, CH_2) and 4.28 (s, CH_2) ppm.

^{13}C NMR ($CDCl_3$): δ_C 14.1 (CH_3), 19.8 (CH_2), 19.9 (CH_2), 20.0 (CH_2), 20.3 (CH_2), 32.7 (CH_2), 32.8 (CH_2), 32.9 (CH_2), 33.0 (CH_2), 33.1 (CH_2), 33.2 (CH_2), 33.3 (CH_2), 60.4 (CH_2), 60.9 (CH_2), 61.9 (CH_2), 62.1 (CH_2), 65.9 (CH_2), 172.5 (C=O), 172.6 (C=O), 172.7 (C=O), 172.8 (C=O), 173.0 (C=O), 173.1 (C=O), 173.2 (C=O), 173.3 (C=O), 176.5 (C=O), 176.7 (C=O) and 176.9 (C=O) ppm.

Acknowledgements

This study was supported by the Portuguese Foundation for Science and Technology (FCT) under the scope of the strategic funding of UID/BIO/04469/2019 unit and BioTecNorte operation (NORTE-01-0145-FEDER-000004) funded by European Regional Development Fund under the scope of Norte2020 - Programa Operacional Regional do Norte. The authors thanks to FCT for funding their scholarship: Jennifer Noro (SFRH/BD/121673/2016), Filipa Gonçalves (SFRH/BD/114684/2016) and Artur Ribeiro (SFRH/BPD/98388/2013). Carla Silva is an investigator FCT (SFRH/IF/

00186/2015). Tarsila Castro thanks the senior position funded by the European Union through the European Regional Development Fund (ERDF) under the Competitiveness Operational Program (BioCell-NanoART = Novel Bio-inspired Cellular Nano-architectures, POC-A1.1.4-E-2015 nr. 30/01.09.2016). Access to computing resources funded by the Project "Search-ON2: Revitalization of HPC infrastructure of UMinho" (NORTE-07-0162-FEDER-000086), cofounded by the North Portugal Regional Operational Programme (ON.2-O Novo Norte), under the National Strategic Reference Framework (NSRF), through the European Regional Development Fund (ERDF), is also gratefully acknowledged.

Conflict of Interest

The authors declare no conflict of interest.

Keywords: PEGylation · esterases · activity · catalysis · polyester

[1] a) J. K. Dozier, M. D. Distefano, *Int. J. Mol. Sci.* **2015**, *16*, 25831–25864 b) B. Yang, Y. Zhao, S. Wang, Y. Zhang, C. Fu, Y. Wei, L. Tao, *Macromolecules* **2014**, *47*, 5607–5612.
[2] C. Silva, M. Martins, S. Jing, J. Fu, A. Cavaco-Paulo, *C. R. Rev. Biotechn.* **2018**, *38*, 335–350.
[3] V. Gaberc-Porekar, I. Zore, B. Podobnik, V. Menart, *Obstacles and pitfalls in PEGylation of therapeutic proteins, Vol. 11*, **2008**.
[4] a) F. M. Veronese, A. Mero, *BioDrugs* **2008**, *22*, 315–329 b) C. J. Fee, J. M. Van Alstine, *Chem. Eng. Sci.* **2006**, *61*, 924–939.
[5] F. M. Veronese, *Biomaterials* **2001**, *22*, 405–417.
[6] H. A. Vandertol-Vanier, R. Vazquez-Duhalt, R. Tinoco, M. A. Pickard, *J. Ind. Microbiol. Biotechnol.* **2002**, *29*, 214–220.
[7] J. I. Lee, S. P. Eisenberg, M. S. Rosendahl, E. A. Chlipala, J. D. Brown, D. H. Doherty, G. N. Cox, *J. Interferon Cytokine Res.* **2013**, *33*, 769–777.
[8] J. Su, J. Noro, A. Loureiro, M. Martins, G. Azoia Nuno, J. Fu, Q. Wang, C. Silva, A. Cavaco-Paulo, *ChemCatChem* **2017**, *9*, 3888–3894.
[9] C. Vilela, A. F. Sousa, A. C. Fonseca, A. C. Serra, J. F. J. Coelho, C. S. R. Freire, A. J. D. Silvestre, *Polym. Chem.* **2014**, *5*, 3119–3141.
[10] Y. Yang, Y. Yu, Y. Zhang, C. Liu, W. Shi, Q. Li, *Process Biochem.* **2011**, *46*, 1900–1908.
[11] a) C. Hedfors, E. Östmark, E. Malmström, K. Hult, M. Martinelle, *Macromolecules* **2005**, *38*, 647–649; b) Y. Yang, W. Lu, J. Cai, Y. Hou, S. Ouyang, W. Xie, R. A. Gross, *Macromolecules* **2011**, *44*, 1977–1985; c) Z. Jiang, C. Liu, W. Xie, R. A. Gross, *Macromolecules* **2007**, *40*, 7934–7943.
[12] K. Mayolo-Deloisa, M. González-González, J. Simental-Martínez, M. Rito-Palomares, *J. Mol. Recognit.* **2015**, *28*, 173–179.
[13] I. W. Hamley, *Biomacromolecules* **2014**, *15*, 1543–1559.
[14] Y. Ikeda, J. Katamachi, H. Kawasaki, Y. Nagasaki, *Bioconjugate Chem.* **2013**, *24*, 1824–1827.
[15] R. Jia, Y. Hu, L. Liu, L. Jiang, B. Zou, H. Huang, *ACS Catal.* **2013**, *3*, 1976–1983.
[16] X. Zhao, S. R. Bansode, A. Ribeiro, A. S. Abreu, C. Oliveira, P. Parpot, P. R. Gogate, V. K. Rathod, A. Cavaco-Paulo, *Ultrason. Sonochem.* **2016**, *31*, 506–511.
[17] X. Zhao, J. Noro, J. Fu, H. Wang, C. Silva, A. Cavaco-Paulo, *Process Biochem.* **2018**, *66*, 82–88.
[18] S. Naik, A. Basu, R. Saikia, B. Madan, P. Paul, R. Chaterjee, J. Brask, A. Svendsen, *J. Mol. Catal. B: Enzym* **2010**, *65*, 18–23.
[19] M. L. C. Cristina, A.-B. Maria Raquel, M. S. C. Joaquim, *Electron. J. Biotechn.* **1998**, *1*, 3.
[20] C. Martinez, A. Nicolas, H. van Tilbeurgh, M. P. Egloff, C. Cudrey, R. Verger, C. Cambillau, *Biochemistry* **1994**, *33*, 83–89.
[21] J. Skjold-Jørgensen, J. Vind, A. Svendsen, M. J. Bjerrum, *Biochemistry* **2014**, *53*, 4152–4160.
[22] a) M. Martinelle, M. Holmquist, K. Hult, *BBA – Lipid Lipid Met.* **1995**, *1258*, 272–276 b) B. Stauch, S. J. Fisher, M. Cianci, *J. Lipid Res.* **2015**, *56*, 2348–2358.
[23] a) T. Zisis, P. L. Freddolino, P. Turunen, M. C. F. van Teeseling, A. E. Rowan, K. G. Blank, *Biochemistry* **2015**, *54*, 5969–5979 b) bN. Willems, M. Lelimousin, J. Skjold-Jørgensen, A. Svendsen, M. S. P. Sansom, *Chem. Phys. Lipids* **2018**, *211*, 4–15 c) cA. Shahid, K. Faez Iqbal, C. Wenwen, R. Abdul, W. Yonghua, *Mol. Simul.* **2018**, *44*, 1520—1528;.
[24] T. Debuissy, E. Pollet, L. Avérous, *Eur. Polym. J.* **2017**, *97*, 328–337.
[25] S. Brännström, M. Finnveden, M. Johansson, M. Martinelle, E. Malmström, *Eur. Polym. J.* **2018**, *103*, 370–377.
[26] Y. Jiang, A. J. J. Woortman, G. O. R. Alberda van Ekenstein, K. Loos, *Polym. Chem.* **2015**, *6*, 5451–5463.
[27] R. Araújo, C. Silva, A. O'Neill, N. Micaelo, G. Guebitz, C. M. Soares, M. Casal, A. Cavaco-Paulo, *J. Biotechnol.* **2007**, *128*, 849–857.
[28] C. Silva, S. Da, N. Silva, T. Matamá, R. Araújo, M. Martins, S. Chen, J. Chen, J. Wu, M. Casal, A. Cavaco-Paulo, *Biotechnol. J.* **2011**, *6*, 1230–1239.
[29] B. Castillo, J. Méndez, W. Al-Azzam, G. Barletta, K. Griebenow, *Biotechnol. Bioeng.* **2006**, *94*, 565–574.
[30] U. Derewenda, L. Swenson, Y. Wei, R. Green, P. M. Kobos, R. Joerger, M. J. Haas, Z. S. Derewenda, *J. Lipid Res.* **1994**, *35*, 524–534.
[31] J. Uppenberg, M. T. Hansen, S. Patkar, T. A. Jones, *Structure* **1994**, *2*, 293–308.
[32] G. Bussi, D. Donadio, M. Parrinello, *J. Chem. Phys.* **2007**, *126*, 014101.
[33] R. Martoňák, A. Laio, M. Parrinello, *Phys. Rev. Lett.* **2003**, *90*, 075503.
[34] a) H. J. C. Berendsen, D. van der Spoel, R. van Drunen, *Comput. Phys. Commun.* **1995**, *91*, 43–56 b) D. v. d. S. M. J. Abraham, E. Lindahl, B. Hess, www.gromacs.org **2017**.
[35] a) W. Huang, Z. Lin, W. F. van Gunsteren, *J. Chem. Theory Comput.* **2011**, *7*, 1237–1243 b) N. Schmid, A. P. Eichenberger, A. Choutko, S. Riniker, M. Winger, A. E. Mark, W. F. van Gunsteren, *Eur. Biophys. J.* **2011**, *40*, 843.
[36] T. Darden, D. York, L. Pedersen, *J. Chem. Phys.* **1993**, *98*, 10089–10092.
[37] B. Hess, *J. Chem. Theory Comput.* **2008**, *4*, 116–122.
[38] S. Miyamoto, P. A. Kollman, *J. Comb. Chem.* **1992**, *13*, 952–962.
[39] J. J. P. Stewart, *J. Mol. Model.* **2007**, *13*, 1173–1213.
[40] G. W. T. M. J. Frisch, H. B. Schlegel, G. E. Scuseria, M. A. Robb, J. R. Cheeseman, G. Scalmani, V. Barone, G. A. Petersson, H. Nakatsuji, X. Li, M. Caricato, A. Marenich, J. Bloino, B. G. Janesko, R. Gomperts, B. Mennucci, H. P. Hratchian, J. V. Ortiz, A. F. Izmaylov, J. L. Sonnenberg, D. Williams-Young, F. Ding, F. Lipparini, F. Egidi, J. Goings, B. Peng, A. Petrone, T. Henderson, D. Ranasinghe, V. G. Zakrzewski, J. Gao, N. Rega, G. Zheng, W. Liang, M. Hada, M. Ehara, K. Toyota, R. Fukuda, J. Hasegawa, M. Ishida, T. Nakajima, Y. Honda, O. Kitao, H. Nakai, T. Vreven, K. Throssell, J. A. Montgomery, Jr., J. E. Peralta, F. Ogliaro, M. Bearpark, J. J. Heyd, E. Brothers, K. N. Kudin, V. N. Staroverov, T. Keith, R. Kobayashi, J. Normand, K. Raghavachari, A. Rendell, J. C. Burant, S. S. Iyengar, J. Tomasi, M. Cossi, J. M. Millam, M. Klene, C. Adamo, R. Cammi, J. W. Ochterski, R. L. Martin, K. Morokuma, O. Farkas, J. B. Foresman, D. J. Fox, *Gaussian, Inc., Wallingford CT, Gaussian 09, n.d. gaussian.com/g09citation/*.
[41] a) A. K. Malde, L. Zuo, M. Breeze, M. Stroet, D. Poger, P. C. Nair, C. Oostenbrink, A. E. Mark, *J. Chem. Theory Comput.* **2011**, *7*, 4026–4037 b) M. Stroet, B. Caron, K. M. Visscher, D. P. Geerke, A. K. Malde, A. E. Mark, *J. Chem. Theory Comput.* **2018**, *14*, 5834–5845.
[42] PyMOL, *The PyMOL Molecular Graphics System, Version 2.0 Schrödinger, LLC., n.d.*
[43] a) J. Noro, R. L. Reis, A. Cavaco-Paulo, C. Silva, *Ultrason. Sonochem.* **2018**, *48*, 51–56 b) J. Noro, A. Loureiro, F. Gonçalves, N. G. Azoia, S. Jung, C. Silva, A. Cavaco-Paulo, *Colloids Surf. B* **2017**, *159*, 259–267.

Manuscript received: March 13, 2019
Revised manuscript received: April 9, 2019
Accepted manuscript online: April 10, 2019
Version of record online: April 30, 2019